(2)

RADC-TR-89-217
Final Technical Report
October 1989

IONOSPHERIC HEATING BY OBLIQUELY TRANSMITTED HIGH POWER RADIO WAVES

Massachusetts Institute of Technology

Ming-Chang Lee

APPROVED FOR PUBLIC RELEASE; DISTRIBUTION UNLIMITED.

ROME AIR DEVELOPMENT CENTER
Air Force Systems Command
Griffiss Air Force Base, NY 13441-5700

This report has been reviewed by the RADC Public Affairs Division (PA) and is releasable to the National Technical Information Services (NTIS) At NTIS it will be releasable to the general public, including foreign nations.

RADC-TR-89-217 has been reviewed and is approved for publication.

APPROVED: Stanford P. Yukon

STANFORD P. YUKON
Project Engineer

APPROVED: John K. Schindler

JOHN K. SCHINDLER
Director of Electromagnetics

FOR THE COMMANDER: John A. Ritz

JOHN A. RITZ
Directorate of Plans & Programs

If your address has changed or if you wish to be removed from the RADC mailing list, or if the addressee is no longer employed by your organization, please notify RADC (EECP) Griffiss AFB NY 13441-5700. This will assist us in maintaining a current mailing list.

Do not return copies of this report unless contractual obligations or notices on a specific document require that it be returned.

UNCLASSIFIED

SECURITY CLASSIFICATION OF THIS PAGE

REPORT DOCUMENTATION PAGE

Form Approved OMB No. 0704-0188

1a. REPORT SECURITY CLASSIFICATION UNCLASSIFIED	1b. RESTRICTIVE MARKINGS N/A
2a. SECURITY CLASSIFICATION AUTHORITY N/A	3. DISTRIBUTION/AVAILABILITY OF REPORT Approved for public release; distribution unlimited.
2b. DECLASSIFICATION/DOWNGRADING SCHEDULE N/A	
4. PERFORMING ORGANIZATION REPORT NUMBER(S) N/A	5. MONITORING ORGANIZATION REPORT NUMBER(S) RADC-TR-89-217
6a. NAME OF PERFORMING ORGANIZATION Massachusetts Institute of Technology 6b. OFFICE SYMBOL (If applicable)	7a. NAME OF MONITORING ORGANIZATION Rome Air Development Center (EECP)
6c. ADDRESS (City, State, and ZIP Code) Plasma Fusion Center Cambridge MA 02139	7b. ADDRESS (City, State, and ZIP Code) Hanscom AFB MA 01731-5000
8a. NAME OF FUNDING/SPONSORING ORGANIZATION Rome Air Development Center 8b. OFFICE SYMBOL (If applicable) EECP	9. PROCUREMENT INSTRUMENT IDENTIFICATION NUMBER F30602-81-C-0193
8c. ADDRESS (City, State, and ZIP Code) Hanscom AFB MA 01731-5000	10. SOURCE OF FUNDING NUMBERS PROGRAM ELEMENT NO: 62702F; PROJECT NO: 4600; TASK NO: 16; WORK UNIT ACCESSION NO: P8

11. TITLE (Include Security Classification)

IONOSPHERIC HEATING BY OBLIQUELY TRANSMITTED HIHG POWER RADIO WAVES

12. PERSONAL AUTHOR(S)
Min-Chang Lee

13a. TYPE OF REPORT	13b. TIME COVERED	14. DATE OF REPORT (Year, Month, Day)	15. PAGE COUNT
Final	FROM Feb 88 TO Dec 88	October 1989	36

16. SUPPLEMENTARY NOTATION
N/A

17. COSATI CODES			18. SUBJECT TERMS (Continue on reverse if necessary and identify by block number)
FIELD	GROUP	SUB-GROUP	
20	14		Oblique Ionospheric Modification

19. ABSTRACT (Continue on reverse if necessary and identify by block number)

Anisotropic effects of ionospheric irregularities on Faraday polarization fluctuations have been investigated. It was found that sheet like irregularities are more effective than rod like irregularities in causing Faraday polarization fluctuations. Measurement of the fluctuation spectrum may be used to diagnose ionospheric irregularities. Nonlinear scattering of HF waves by ionospheric irregularities has also been investigated. It was shown that HF ionospheric heating can be further enhanced by nonlinear scattering of VLF waves. Artificial spread F caused by ionospheric heating with either vertically or obliquely incident high power HF waves has been investigated by ray-tracing simulation codes.

20. DISTRIBUTION/AVAILABILITY OF ABSTRACT ☒ UNCLASSIFIED/UNLIMITED ☐ SAME AS RPT. ☐ OTIC USERS	21. ABSTRACT SECURITY CLASSIFICATION UNCLASSIFIED
22a. NAME OF RESPONSIBLE INDIVIDUAL Stanford P. Yukon	22b. TELEPHONE (Include Area Code) (617) 377-2985 22c. OFFICE SYMBOL RADC (EECP)

DD Form 1473, JUN 86 Previous editions are obsolete.

SECURITY CLASSIFICATION OF THIS PAGE
UNCLASSIFIED

Final Report to Rome Air Development Center for Sponsored Research in "Ionospheric Heating by Obliquely Transmitted High Power Radio Waves " during February 3 - December 3, 1988. Prepared by

Dr. Min-Chang Lee
Principal Investigator

1. Introduction

Continued research under the sponsorship of RADC has been actively conducted at Massachusetts Institute of Technology in ionospheric heating by obliquely transmitted high power radio waves. During the period of February 3 - December 3, 1988, research effort centered on (1) analysis of induced ionospheric effects , (2) diagnosis of oblique heating effects by ionosondes, and (3) planning of the ECRS-Bermuda *oblique heating experiment* with RADC.

Because of the oblique wave propagation in the ionosphere, resonant wave-plasma interactions which require strict frequency and wave vector matching relations are not expected to occur. These resonant wave-plasma interaction processes, which can generate short-scale (typically, meter-scale) ionospheric density irregularities play important roles in the vertical heating experiments. It is, however, expected that large-scale (typically, hundred meter-scale) ionospheric density irregularities are able to be excited by thermal filamentation/self-focusing instabilities. These large-scale instabilities can produce prominent ionospheric effects along the wave path in a large ionospheric region. In the following, we will briefly report our analysis of these heater wave-induced ionospheric disturbances and their effects on radio propagation.

2. Heater wave-induced ionospheric irregularities

Ionospheric density irregularities generated by filamentation instabilities can have two independent wave-vector directions. The irregularities excited by the o mode heater waves are field aligned and have wave-vectors pointing to the direction perpendicular to the meridian plane. By contrast, the irregularities excited by the x mode heater waves are

polarized in the meridian plane and are, in general, not field aligned. The field aligned nature of induced ionospheric irregularities, however, is eventually established to reduce the diffusion damping along the geomagnetic field.

As illustrated in Figure 1, the radio signals transmitted vertically from an ionosonde can have two different types of ray trajectories in the presence of ionospheric density irregularities. The reflection heights of these ray trajectories are significantly different from those of ray trajectories in the absence of heater induced ionospheric irregularities. The fluctuation of reflection heights, then, gives rise to the spread F echoes on the ionograms. It can be shown that irregularities polarized within the meridian plane can cause spread F, while those polarized in planes perpendicular to the meridian planes can not.

We have developed ray tracing codes to simulate the artificial spread F caused by ionospheric heating with either vertically or obliquely transmitted high power radio waves. A linear ionospheric density profile is adopted in the ray tracing codes. Further, we also develop a ray tracing code for radial density profile which represents the typical inhomogeneous laboratory plasmas. This work is part of our planned laboratory study of nonlinear wave-plasma interactions which can simulate the oblique ionospheric heating experiments. Two students, Dan Moriarty and Larry McKay, are working with Dr. Lee on ray tracing study of radio propagation in perturbed ionosphere for their thesis research. The results of the research will be reported later.

3. Anisotropic effects of ionospheric irregularities

The anisotropic effects of ionospheric irregularities on Faraday polarization fluctuations have been investigated by Dr. Lee with a student, S.V. Nghiem. This work extends the earlier theory of Lee et al [1982], explaining the Faraday polarization fluctuations of satellite beacon signals at 136 MHz. In the previous work, isotropic correlation functions were assumed for the ionospheric density fluctuations for simplicity. However, ionospheric density irregularities have prominent anisotropic nature, namely, they elongate along the earth's magnetic field to reduce diffusion damping. Rod-like and sheet-like are the two forms of ionospheric irregularities commonly seen in the ionosphere. Sheet-like ionospheric irregularities are observed in the auroral oval, while rod-like irregularities at higher and lower latitudes. The different geometric effects of these ionospheric irregularities can be exhibited in the scintillation measurements of radio signals.

Striking anisotropic effects of ionospheric irregularities are found on the Faraday polarization fluctuations of linearly polarized radio waves, propagating along the earth's magnetic field. Nevertheless, if the wave propagation angle is not small (say, greater than 5 degrees), the anisotropic effects of rod-like irregularities weaken significantly while

those of sheet-like irregularities remain prominent. In general, the sheet-like ionospheric irregularities are more effective than the rod-like irregularities in causing the Faraday polarization fluctuation of radio waves.

The present work can be based on to develop a radio technique for diagnosing the ionospheric irregularities induced by the obliquely transmitted radio waves. As shown in Figure 2, a linearly polarized diagnostic radio wave with a slightly less frequency is transmitted along the same path of the heater wave. Then, the heater wave-induced ionospheric irregularities will cause the polarization fluctuations of the diagnostic wave. Further, the nature of the induced ionospheric irregularities can also be deduced on the basis of the present theory. A preprint of the paper is attached as Appendix A of this report.

4. Nonlinear scattering of radio waves

Nonlinear scattering of radio waves by ionospheric irregularities was also investigated. The details of the research were presented in last year's report to RADC. This process has been based on to interpret the observed spectral broadening of VLF radio waves traversing the ionosphere. In addition, it has been shown that ionospheric heating by HF heater waves can be further enhanced by the nonlinear scattering of VLF waves. Two papers describing results of the research were recently published in technical journals by Dr. Lee and his students. They are included in this report as Appendices B and C.

A-1

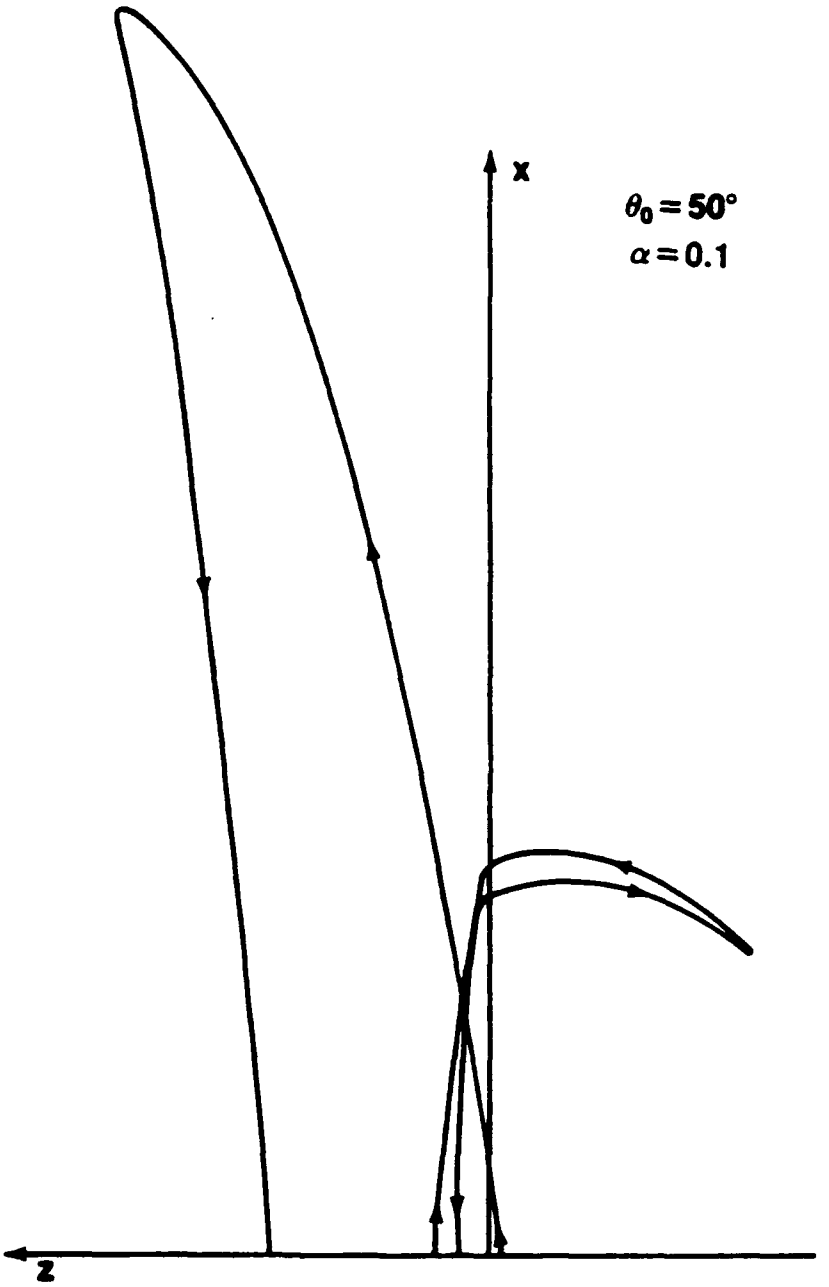

Figure 1. Radio signals transmitted from an ionosonde have two different ray trajectories in the presence of ionospheric irregularities.

Oblique Heating Experiments

a. field experiments

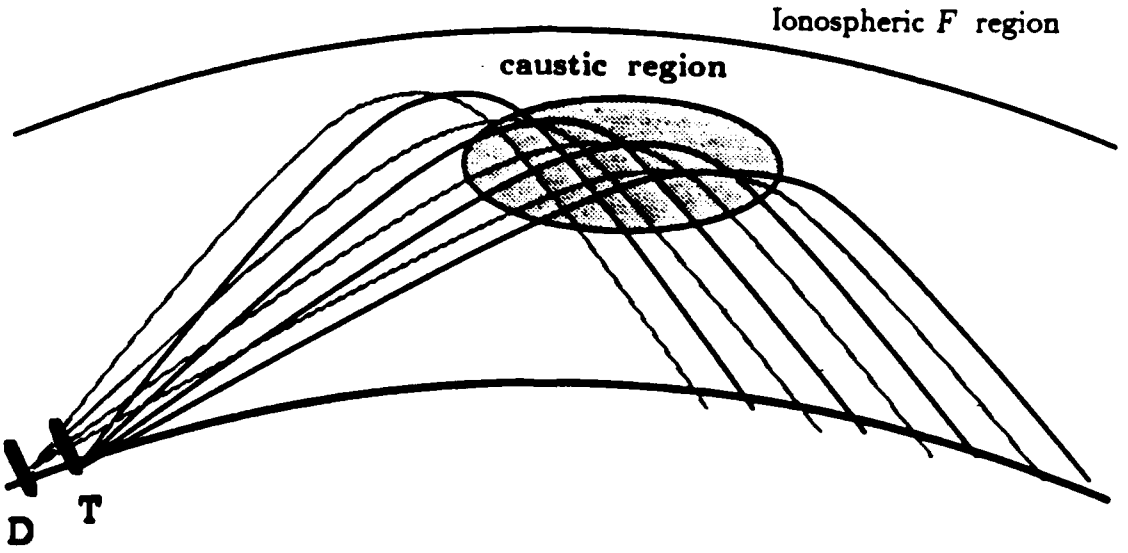

D : Diagnostic radio wave

T : Heater wave

Figure 2. Schematic illustration of oblique ionospheric heating experiments. A diagnostic wave with a frequency slightly less than the heater wave frequency is transmitted along the same path as the heater wave.

Appendix A

Anisotropic Effects of Ionospheric Irregularities on Faraday Polarization Fluctuations

Abstract

The previous model [Lee et al., 1982] of the Faraday polarization fluctuations (FPF) is extended after taking into account the anisotropic nature of the commonly observed, rod-like and sheet-like ionospheric irregularities. Striking anisotropic effects are seen in the longitudinal radio propagation. However, if the wave propagation angle is not small (say greater than 5°), the anisotropic effects of rod-like irregularities weaken significantly while those of sheet-like irregularities remain prominent. In general, the sheet-like ionospheric irregularities are more effective than the rod-like ionospheric irregularities in causing the FPF of radio waves. It is expected that intense FPF of VHF radio signals can be observed not only near the equatorial anomaly but also in the auroral region.

1. Introduction

The phenomenon of Faraday Polarization Fluctuations (FPF) has been observed with low-orbit satellite beacon signals transmitted at the frequencies of 20, 40, and 54 MHz, and also with geostationary satellite signals at 136 MHz [Lee et al., 1982 and references therein]. It results from the diffractive scattering of radio waves by ionospheric density irregularities [Yeh and Liu, 1967; Lee et al., 1982; Bhattacharyya and Rastogi, 1987]. Ionospheric irregularities characterized by power-law spectra can cause the FPF of radio signals in a broad range of frequencies (including the VHF signals). By contrast, those with Gaussian spectra can only give rise to the FPF of radio waves at frequencies up to the HF band.

In the previous work, the ionospheric irregularities are assumed to be isotropic for simplicity, and modelled by correlation functions having the same correlation length in all directions. In fact, ionospheric irregularities elongate along the earth's magnetic field. They are highly anisotropic because their scale lengths along the geomagnetic field are much greater than those across the geomagnetic field. Rod-like and sheet-like are the two forms of density irregularities commonly seen in the ionosphere. The different geometric effects of these ionospheric irregularities can be exhibited in the scintillation measurements of radio signals [Costa et al., 1988].

The purpose of the present work is to investigate the anisotropic effects of ionospheric irregularities on the Faraday polarization fluctuations (FPF) of radio waves. The analysis of FPF presented in the next two sections is done for both the rod-like and sheet-like ionospheric irregularities. Discussion and comparison of the prominent anisotropic effects introduced by these ionospheric irregularities on the FPF are subsequently given.

2. Variance of the Faraday Polarization Fluctuations

Consider the propagation of a linearly polarized radio signal through the ionosphere modelled as a plasma slab of mean density N and thickness D. A Cartesian system of

coordinates, as illustrated in Figure 1, is chosen at the transmitter $S(0,0,0)$ with its z axis along the signal path from the transmitter to the receiver $R(0,0,Z_0)$ on the ground. Ionospheric density irregularities, denoted by $\Delta\bar{f}_N^2$, fluctuate about a mean value $<\bar{f}_N^2>$ where $\bar{f}_N$ is the ratio of the ambient plasma frequency to the signal frequency. The variance of Faraday polarization fluctuations has been formulated for single, small-angle forward scattering as

$$\langle |I|^2 \rangle = \frac{{Z_o}^2}{16\pi^2}\frac{\omega^4}{c^4}\int_V d\vec{r}_1 \int_V d\vec{r}_2 \frac{C(\vec{r}_1-\vec{r}_2)}{z_1 z_2 (Z_0-z_1)(Z_0-z_2)} \cos\Big[\frac{k({x_1}^2+{y_1}^2)Z_0}{2z_1(Z_0-z_1)} - \frac{k({x_2}^2+{y_2}^2)Z_0}{2z_2(Z_0-z_2)}\Big] \sin\Big[\frac{\epsilon k({x_1}^2+{y_1}^2)Z_0}{2z_1(Z_0-z_1)}\Big] \sin\Big[\frac{\epsilon k({x_2}^2+{y_2}^2)Z_0}{2z_2(Z_0-z_2)}\Big] \tag{1}$$

where $C(\vec{r}_1-\vec{r}_2) = \langle(\Delta\bar{f}_N^2(\vec{r}_1))(\Delta\bar{f}_N^2(\vec{r}_2))^*\rangle$ is the correlation function of the density irregularities (see equation (19) in Lee et al. [1982]).

3. Rod-like ionospheric irregularities

The anisotropy of ionospheric irregularities can be accounted for by a longer correlation length in the direction parallel to the magnetic field and a shorter correlation length in the perpendicular direction. Ionospheric irregularities with a rod-like configuration can be reasonably expressed by the following correlation function

$$C(\vec{r}_1'-\vec{r}_2') = \langle(\Delta\bar{f}_N^2)^2\rangle \exp\left(\frac{|x_1'-x_2'|}{\ell_\perp}\right)\exp\left(\frac{|y_1'-y_2'|}{\ell_\perp}\right)\exp\left(\frac{|z_1'-z_2'|}{\ell_\parallel}\right) \tag{2}$$

where $\langle(\Delta\bar{f}_N^2)^2\rangle$ corresponds to the mean squared density fluctuations, $\ell_\perp$ ($\ell_\parallel$) is the correlation length across (along) the earth's magnetic field. The system of the prime coordinates is designated in Figure 2.

Since equation (1) is written in the unprime coordinates, the correlation function (2) needs also be expressed in the same coordinates. The prime and unprime coordinates are related by

$$\begin{pmatrix} x' \\ y' \\ z' \end{pmatrix} = \begin{pmatrix} \sin\psi & -\cos\psi & 0 \\ \cos\theta\cos\psi & \cos\theta\sin\psi & -\sin\theta \\ \sin\theta\cos\psi & \sin\theta\sin\psi & \cos\theta \end{pmatrix} \begin{pmatrix} x \\ y \\ z \end{pmatrix} \tag{3}$$

It is convenient to make the following coordinate transformation to carry out the integrations in equation (1) :

$$\begin{aligned} \xi &= x_1 - x_2 \qquad \eta = y_1 - y_2 \qquad \zeta = z_1 - z_2 \\ 2X &= x_1 + x_2 \qquad 2Y = y_1 + y_2 \qquad 2Z = z_1 + z_2 \end{aligned} \tag{4}$$

After the above transformation, the correlation function has the form of

$$\begin{aligned} C(\xi,\eta,\zeta) =& \langle(\Delta \bar{f}_N^2)^2\rangle \exp\left[\frac{1}{\ell_\perp}|\xi\sin\psi - \eta\cos\psi|\right] \\ & \cdot \exp\left[\frac{1}{\ell_\perp}|\xi\cos\theta\cos\psi + \eta\cos\theta\sin\psi - \zeta\sin\theta|\right] \\ & \cdot \exp\left[\frac{1}{\ell_\parallel}|\xi\sin\theta\cos\psi + \eta\sin\theta\sin\psi + \zeta\cos\theta|\right] \end{aligned} \tag{5}$$

Integrations of equation (1) over x and y with infinite limits yield

$$\begin{aligned} \langle|I|^2\rangle =& \frac{k^2}{16\pi(1- < \bar{f}_N^2 >)^2} \int_a^{a+D\sec\chi} dZ \\ & \cdot \int_{-D\sec\chi}^{D\sec\chi} d\zeta \int_{-\infty}^{\infty} d\eta \int_{-\infty}^{\infty} d\xi C(\xi,\eta,\zeta) \\ & \cdot \sum_t G(t)\sin\left[G(t)(\xi^2+\eta^2)\right] \end{aligned} \tag{6}$$

where $G(t)$ and $\sum_t$ are defined as follows

$$G(t) = Z_0 k\left[2\zeta(2Z - Z_0) + 4t(ZZ_0 - Z^2 - \zeta^2/4)\right]^{-1} \tag{7}$$

$$\sum_t h(t) = 2h(0) - h(\epsilon) - h(-\epsilon) \tag{8}$$

To simplify the integrations in equation (6), (ξ,η,ζ) is transformed into (u,v,w). They are related by the same transformation tensor in equation (3). This transformation converts equation (6) into

$$\begin{aligned} \langle|I|^2\rangle =& \frac{k^2\langle(\Delta \bar{f}_N^2)^2\rangle}{16\pi(1- < \bar{f}_N^2 >)^2} \int_a^{a+D\sec\chi} dZ \int_{v_a}^{v_b} dv \\ & \cdot \int_{-\infty}^{\infty} dw \exp\left(-\frac{|w|}{\ell_\parallel}\right) \int_{-\infty}^{\infty} du \exp\left(-\frac{|u|+|v|}{\ell_\perp}\right) \\ & \cdot \sum_t |G(t)|\sin\left[|G(t)|((v\cos\theta + w\sin\theta)^2 + u^2)\right] \end{aligned} \tag{9}$$

where $v_a = w\cot\theta - D\sec\chi\csc\theta$, $v_b = w\cot\theta + D\sec\chi\csc\theta$, and all the ζ's in (7) have been replaced by $(-v\sin\theta + w\cos\theta)$.

To carry out the integrations in equation (9) further, the following transformations are made:

$$\begin{aligned} V &= v\cos\theta \qquad & W &= w\sin\theta \\ V+W &= s \qquad & V-W &= p \end{aligned} \tag{10}$$

This set of transformations renders the integration over p trivial. The result after the integration over p is

$$\begin{aligned} \langle|I|^2\rangle =& \frac{k^2\langle(\Delta\bar{f}_N^2)^2\rangle}{4\pi(1-<\bar{f}_N^2>)^2}\int_a^{a+D\sec\chi} dZ \\ & \cdot\int_0^\infty du\exp\left(-\frac{u}{\ell_\perp}\right)\left[\frac{\sin^2\theta}{{\ell_\perp}^2}-\frac{\cos^2\theta}{{\ell_\parallel}^2}\right]^{-1}\int_0^\infty ds \\ & \cdot\left[\frac{\sin\theta}{\ell_\perp}\exp\left(-\frac{|s|}{\ell_\parallel\sin\theta}\right)-\frac{\cos\theta}{\ell_\parallel}\exp\left(-\frac{|s|}{\ell_\perp\cos\theta}\right)\right] \\ & \cdot\sum_t|G(t)|\sin\left[|G(t)|(u^2+s^2)\right] \end{aligned} \tag{11}$$

The integrations over u and s can be carried out exactly. Then, the integration over Z can simply be approximated by the product of the interval of integration and the integrand wherein all the Z's are set equal to Z_m, the distance between the transmitter and the mean height of the plasma slab.

Finally, the variance of the Faraday rotation fluctuations is obtained as

$$\begin{aligned} \langle|I|^2\rangle =& \frac{Ak^2<\bar{f}_N^2>^2}{4(1-<\bar{f}_N^2>)^2}\langle(\Delta N/N)^2\rangle \\ & \cdot D\sec\chi\left(\frac{\sin^2\theta}{{\ell_\perp}^2}-\frac{\cos^2\theta}{{\ell_\parallel}^2}\right)^{-1} \end{aligned} \tag{12}$$

where

$$\begin{aligned} A =& \frac{\sin\theta}{\ell_\perp}[1-2F_s(L)F_c(L_s)-2F_c(L)F_s(L_s)] \\ & -\frac{\cos\theta}{\ell_\parallel}[1-2F_s(L)F_c(L_c)-2F_c(L)F_s(L_c)] \end{aligned} \tag{13}$$

in which $L^2 = \frac{\epsilon d}{(k{\ell_\perp}^2)}$, ${L_s}^2 = \frac{\epsilon d}{(k{\ell_\parallel}^2\sin^2\theta)}$, ${L_c}^2 = \frac{\epsilon d}{(k{\ell_\perp}^2\cos^2\theta)}$, d is the mean height of the density irregularities, and the functions $F_s(x)$ and $F_c(x)$ are defined by equations (14) and

(15), respectively.

$$F_s(x) = \frac{1}{2}[\cos(x^2) + \sin(x^2)] - [\cos(x^2)C(x) + \sin(x^2)S(x)] \tag{14}$$

$$F_c(x) = \frac{1}{2}[\cos(x^2) - \sin(x^2)] - [\cos(x^2)S(x) - \sin(x^2)C(x)] \tag{15}$$

where $S(x)$ and $C(x)$ are the Fresnel sine and the Fresnel cosine functions, respectively.

The expression for FPF variance in (12) can be very much simplified because the arguments of the functions $F_s(x)$ and $F_c(x)$ are very small with the adopted ionospheric parameters discussed in the next section. Therefore, $F_s(x)$ and $F_c(x)$ can be expanded into power series, and terms of the order of x are kept to yield the result

$$\langle |I|^2 \rangle = \frac{k < \bar{f}_N^2 >^2 (\epsilon k d)^{1/2} D \sec\chi}{5(1 - < \bar{f}_N^2 >)^2 [\sin\theta + \left(\ell_\perp / \ell_\parallel\right) \cos\theta]} \langle (\Delta N/N)^2 \rangle \tag{16}$$

which is valid for $\ell_\parallel \sin\theta \gg \sqrt{(\epsilon d/k)}$ and $\ell_\perp \cos\theta \gg \sqrt{(\epsilon d/k)}$. The term associated with the $(\ell_\perp/\ell_\parallel)$ in (16) accounts for the anisotropic effects of rod-like irregularities on the FPF. In the case of exactly longitudinal propagation, the FPF variance can be calculated from (11) by setting $\theta = 0°$. For $\ell_\perp \cos\theta \gg \sqrt{(\epsilon d/k)}$, the result is

$$\langle |I|^2 \rangle = \frac{k < \bar{f}_N^2 >^2 (\epsilon k d)^{1/2} D \sec\chi}{5(1 - < \bar{f}_N^2 >)^2} \left(\ell_\parallel / \ell_\perp\right) \langle (\Delta N/N)^2 \rangle \tag{17}$$

4. Sheet-like ionospheric irregularities

Sheet-like ionospheric irregularities are seen in the auroral oval, while rod-like irregularities at higher and lower latitudes [e.g., Aarons, 1982]. Sheet-like irregularities can be represented by the correlation function in the form of

$$C(\vec{r}_1' - \vec{r}_2') = \langle (\Delta \bar{f}_N^2)^2 \rangle \exp\left(-\frac{|x_1' - x_2'|}{\ell_\perp}\right) \exp\left(-\frac{|y_1' - y_2'|}{\ell_\parallel}\right) \exp\left(-\frac{|z_1' - z_2'|}{\ell_\parallel}\right) \tag{18}$$

These sheets may coincide with the meridian plane or a plane which is orthogonal to the meridian plane. In the former case, the $y'z'$ plane represents the meridian plane and the x' axis points to the east- west direction. Whereas, in the latter case, the x' axis is along the north-south direction and the $y'z'$ plane intersects the meridian plane at right angles.

The corresponding variances of the FPF caused by the sheet-like irregularities are found to be

$$< |I|^2 >= \frac{k < \bar{f}_N^2 >^2 (\epsilon k d)^{1/2} D \sec\chi}{5(1- < \bar{f}_N^2 >)^2(\sin\theta + \cos\theta)} \left(\frac{\ell_\parallel}{\ell_\perp}\right) \langle \left(\frac{\Delta N}{N}\right)^2 \rangle \tag{19}$$

and, for the longitudinal propagation ($\theta = 0°$),

$$< |I|^2 > \simeq \frac{k < \bar{f}_N^2 >^2 (\epsilon k d)^{1/2} D \sec\chi}{5(1- < \bar{f}_N^2 >)^2} \left(\ell_\parallel/\ell_\perp\right) < (\Delta N/N)^2 > \tag{20}$$

where $\ell_\parallel \gg \ell_\perp$ is assumed. Compare equations (19) and (20) with (16) and (17), one can see the distinctive anisotropic effects introducd by the sheet-like and rod-like ionospheric irregularities on the FPF of radio waves. It is evident from (16) that, as $\sin\theta > (\ell_\perp/\ell_\parallel)\cos\theta$ [e.g., $\theta > 5.7°$ for $\ell_\perp/\ell_\parallel = 0.1$], the anisotropic effect of rod-like ionospheric irregularities is no longer prominent for large propagation angles. By contrast, the anisotropic effect of sheet-like irregularities does not depend upon the propagation angles strongly according to (19). The most prominent anisotropic effects of ionospheric irregularities are seen in the longitudinal radio propagation. Further, both the rod-like and sheet-like irregularities exhibit the same effects on the longitudinal wave propagation.

5. Discussion and Conclusion

We have extended the previous model of the Faraday Polarization Fluctuations (FPF) by taking into account the anisotropy of ionospheric irregularities. The anisotropic effects of the commonly observed, rod-like and sheet-like ionospheric irregularities on the FPF of radio waves are examined. The striking anisotropic effects of both types of ionospheric irregularities are expected for the longitudinal radio propagation.

However, if the wave propagation angle (θ) is not small (say, $\theta > 5°$), the anisotropic effects of rod-like irregularities weaken significantly, while those of sheet-like irregularities remain prominent. When $(\ell_\perp/\ell_\parallel)\cos\theta$ is much less than $\sin\theta$, equation (16) reduces to a form similar to equation (27) of Lee et al. [1982]. Hence, the refractive wave scattering by rod-like ionospheric irregularities for a large propagation angle can be adequately described by the isotropic random- medium model of Lee et al. [1982].

The primary distinction between equation (27) of Lee et al. [1982] and equation (19) is the large factor, $(\ell_{\|}/\ell_{\perp}) \sim O(1)$ which characterizes the anisotropic effects of sheet-like irregularities. Because of this large factor, the ionospheric conditions for the occurrence of FPF can be significantly relaxed. For instance, the FPF caused by the sheet-like ionospheric irregularities requires less density fluctuation, *and/or* background plasma density to occur. We, therefore, conclude that the sheet-like irregularities are more effective than the rod-like irregularities in causing the FPF of radio waves. Since the sheet-like irregularities appear in the auroral oval while the rod-like irregularities at higher and lower latitudes [Aarons, 1982], the present work predicts that intense FPF of VHF signals can be observed not only near the equatorial anomaly but also in the auroral region.

Acknowledgements. This work was supported by the NASA Grant NAG 5-1055, Lincoln Lab grant (under the Air Force contract to Lincoln Lab # F19628-80-C-0002), and the RADC contract through the Southeastern Center for Electrical Engineering Education.

References

Aarons, J., Global morphology of ionospheric scintillations, *Proc. IEEE*, **70**, 360-378, *1982.*

Bhattacharyya, A. and R. G. Rastogi, Faraday polarization fluctuations of VHF geostationary satellite signals near the geomagnetic equator, *J. Geophys. Res.*, **92**, 8821-8826, *1987.*

Costa, E., P. F. Fougere, and S. Basu, Cross-correlation analysis and interpretation of spaced-receiver measurements, *Radio Sci.*, **23**, 141-162, *1988.*

Lee, M.C., A. Das Gupta, J.A. Klobuchar, S.Basu, and S.Basu, Depolarization of VHF geostationary satellite signals near the equatorial anomaly crests, *Radio Sci.*, **17**, 399-409, *1982.*

Yeh, K.C., and C.H. Liu, Wave propagation in a random medium with anisotropic background, *IEEE Trans. Antennas Propag.* A-P 15, 539-542, *1967.*

Figure Captions

Figure 1. Geometry of the transionospheric radio propagation in the presence of ionospheric density irregularities.

Figure 2. Illustration of anisotropic ionospheric density irregularities.

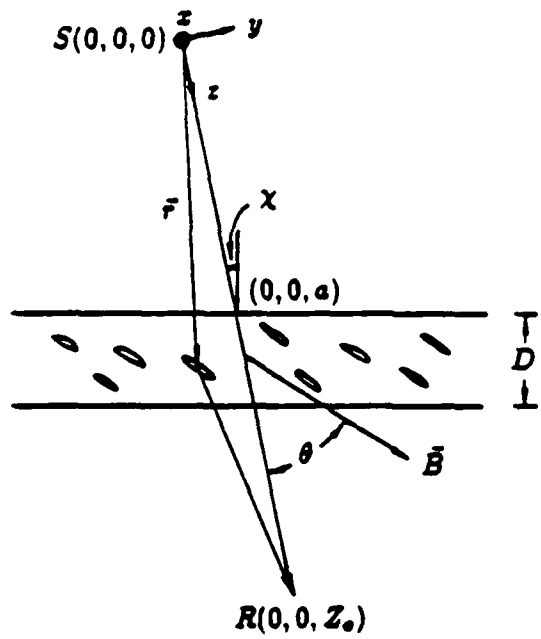

Figure 1.

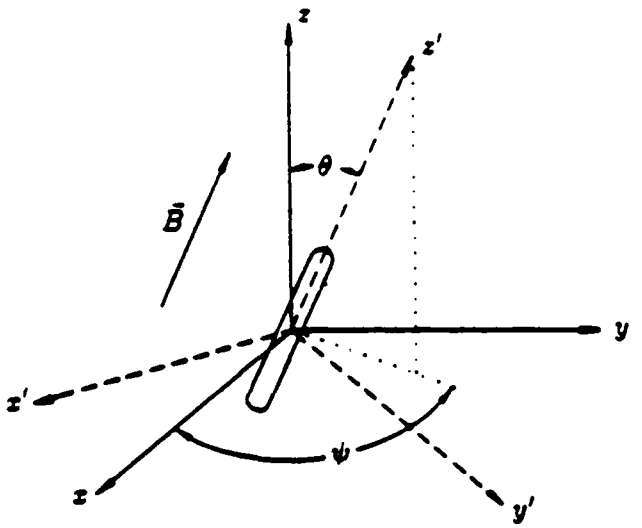

Figure 2.

JOURNAL OF GEOPHYSICAL RESEARCH, VOL. 93, NO. A12, PAGES 14,683–14,687, DECEMBER 1, 1988

Appendix B

Spectral Broadening of VLF Radio Signals Traversing the Ionosphere

K. M. GROVES AND M. C. LEE

Plasma Fusion Center, Massachusetts Institute of Technology, Cambridge

S. P. KUO

Weber Research Institute, Polytechnic University, Farmingdale, New York

Nearly monochromatic signals at 13.6 kHz ±1 Hz injected from a ground-based VLF transmitter can experience a bandwidth expansion as high as 1% (~ 100 Hz) of the incident wave frequency as they traverse the ionosphere and reach satellite altitudes in the range of 600–3800 km (Bell et al., 1983). The off-carrier components, having electrostatic nature, are believed to be induced lower hybrid wave modes. We investigate two different source mechanisms that can potentially result in the observed spectral broadening of injected monochromatic VLF waves. One is the nonlinear scattering of VLF signals by ionospheric density fluctuations that renders the nonlinear mode conversion of VLF waves into lower hybrid waves. These electrostatic modes result when the injected VLF waves are scattered by ionospheric density fluctuations with scale lengths less than $\sqrt{2}\pi(c/\omega_{pe})(\Omega_e/\omega_o)^{1/2} \sim 2$ km in the upper ionosphere, where c, ω_{pe}, Ω_e, and ω_o are the speed of light in vacuum, the plasma frequency, the electron cyclotron frequency, and the VLF wave frequency, respectively. In the absence of ionospheric irregularities, a second mechanism that involves a parametric instability can excite the lower hybrid waves (Lee and Kuo, 1984). This process tends to produce a spectrally broadened transmitted pulse with peaks at a discrete set of frequencies on both sides of the nominal carrier frequency. By contrast, the nonlinear scattering mechanism generates single-peaked spectra centered at the carrier frequency. Both types of spectra were observed in the experiments. Therefore, the two suggested source mechanisms contribute additively to the observed spectral broadening of injected VLF waves.

1. INTRODUCTION

Nearly monochromatic signals at 13.6 kHz ± 1 Hz injected from a ground-based VLF transmitter were recently observed to experience bandwidth expansion as they traversed the ionosphere and reached the satellite altitudes in the range of 600–3800 km [*Bell et al.*, 1983]. This expansion of bandwidth, which results in a proportional increase in signal-to-noise ratio, may be as large as 1% (~ 100 Hz) of the carrier frequency, and the off-carrier components are thought to be electrostatic in nature [*Inan and Bell, 1985*]. They occur only in the presence of impulsive VLF hiss and/or a lower hybrid resonance (LHR) noise band with an irregular cutoff frequency, and only for signals whose frequencies exceed the LHR frequency at the satellite location. Based on these observed characteristics of the spectrally broadened transmitter signals, one may suspect the off-carrier components to be either electrostatic whistler wave modes or lower hybrid wave modes.

The linear scattering source mechanism producing quasi-electrostatic whistler wave modes was first suggested by *Bell et al.* [1983], who hypothesized the creation of the required ionospheric density fluctuations by precipitating, low-energy (< 1 keV) electrons. Such precipitation events have been accompanied by both VLF hiss and irregular LHR noise bands [*McEwen and Barrington*, 1967; *Laaspere et al.*, 1971; *Gurnett and Frank*, 1972]. *Bell et al.* [1983] then speculate that the broadening of the transmitted pulse spectrum results from the scattering of the initial signals from the precipitation-induced density fluctuations and the subsequent coupling into quasi-electrostatic whistler wave modes of short wavelength. The Doppler shift associated with these short-wavelength modes is estimated to be large enough to produce the bandwidth expansion of the signals measured on a moving satellite.

However, we interpret the off-carrier components of the spectrally broadened transmitter signals to be lower hybrid wave modes. The main reason is that the lower hybrid wave modes (eigenmodes of ionospheric plasmas) experience less spatial attenuation than the quasi-electrostatic whistler wave modes (quasi-modes of ionospheric plasmas) during propagation from the source regions to the satellite location. Two source mechanisms are proposed, whereby the transmitted VLF waves can potentially produce the lower hybrid waves. One mechanism comparable to that of *Bell et al.* [1983], termed "nonlinear scattering process," occurs in the presence of ionospheric density irregularities. The other one, by contrast, does not require the presence of ionospheric irregularities. It is a parametric instability that, excited by intense enough VLF waves, can generate lower hybrid waves and ionospheric irregularities concomitantly [*Lee and Kuo*, 1984].

The first mechanism, presented in section 2, differs from that of Bell et al. The newly proposed nonlinear process is a scattering of the whistler mode VLF signals by preexisting density fluctuations that render a mode conversion to lower hybrid waves, instead of a linear process that couples energy into the quasi-electrostatic branch of the whistler mode. We formulate a theory of VLF wave scattering off

Paper number 88JA03332.
0148-0227/88/88JA-03332$05.00

ionospheric irregularities, showing how this process depends upon the local fractional density fluctuations, the ratio of their scale lengths to the VLF wavelength, etc. The scattering of VLF waves by ionospheric density fluctuations generally causes elliptically polarized modes. The induced elliptically polarized modes, however, may be predominantly electrostatic under certain ionospheric conditions.

The second mechanism, described in section 3, produces a spectrally broadened signal via a parametric instability [*Lee and Kuo*, 1984]. The injected VLF wave, if intense enough, parametrically excites a magnetic field-aligned purely growing mode together with two sidebands of lower hybrid waves. The parametric excitation process requires the frequency and wave vector matching relations to be satisfied. The two lower hybrid wave sidebands are characterized by their wave vectors which are the sum and difference of the wave vectors of the whistler pump and the purely growing mode, respectively.

The lower hybrid waves generated by either of the two proposed mechanisms can have wavelengths much shorter than that of the incident VLF waves. In other words, much greater wave numbers are introduced by the suggested source mechanisms for the injected VLF waves that, essentially, become electrostatic modes. These electrostatic plasma modes with large wave numbers, detected by satellites moving across the geomagnetic field, give rise to Doppler shifts that were observed as the broadened spectra (i.e., off-carrier components) of the injected VLF waves. The preliminary results were presented in *Lee et al.* [1986].

2. NONLINEAR WAVE SCATTERING

Theory

A monochromatic VLF wave transmitted from a ground-based station into space has been observed to change from linear into circular polarization (i.e., whistler mode). If a ducted whistler wave mode, propagating exactly along the geomagnetic field, is considered for simplicity, the wave electric field may be represented as

$$\mathbf{E} = E_o(\hat{\mathbf{x}} + i\hat{\mathbf{y}})\exp[i(k_o z - \omega_o t)] \tag{1}$$

where the z axis has been taken along the geomagnetic field lines, ω_o is the transmitted wave frequency, and $\mathbf{k}_o$ the associated wave vector, assumed to be along the z axis as illustrated in Figure 1*a*. Propagating into the ionosphere with no irregular structure, the whistler wave satisfies the electromagnetic wave equation

$$\nabla^2\mathbf{E}_o - \frac{1}{c^2}\frac{\partial^2}{\partial t^2}\mathbf{E}_o = \mu_o\frac{\partial}{\partial t}\mathbf{j}_o \tag{2}$$

where $\mathbf{j}_o$ is the uniform oscillatory current driven by the incident wave field in the ionospheric plasma,

$$\mathbf{j}_o = \frac{ie^2N_o\mathbf{E}_o}{m(\omega_o - \Omega_e)}$$

and e, N_o, m, and Ω_e are the electron charge, uniform background plasma density, electron mass, and the unsigned electron cyclotron frequency, respectively. In the presence of field-aligned ionospheric density irregularities, the scattered wave, allowing for electrostatic modes, can be described by

$$\nabla(\nabla\cdot\mathbf{E}_s) - \nabla^2\mathbf{E}_s + \frac{1}{c^2}\frac{\partial^2}{\partial t^2}\mathbf{E}_s = -\mu_o\frac{\partial}{\partial t}\delta\mathbf{j}_s \tag{3}$$

where $\delta\mathbf{j}_s$ is the nonuniform current induced by the interaction of the whistler wave field with the density irregularities. We take the x axis along the direction of the density irregularities which are assumed to be of the form

$$\delta n = \delta\tilde{n}\exp[ikx] \tag{4}$$

depicted graphically in Figure 1*b*. The nonuniform current $\delta\mathbf{j}_s$ can then be expressed as

$$\delta\mathbf{j}_s = -e(N_o\delta\mathbf{v} + \frac{\delta n}{N_o}\mathbf{j}_o) \tag{5}$$

where $\delta\mathbf{v}$ is the induced velocity perturbation. The scattered wave field has the general form of

$$\mathbf{E}_s = [\hat{\mathbf{x}}E_x + i\hat{\mathbf{y}}E_y]\exp[i(k_o z - \omega_o t)] \tag{6}$$

Solving the wave equation together with the electron momentum equation, the scattered wave field is found to be elliptically polarized,

$$\mathbf{E}_s = E_o(\delta n/N_o)[\hat{\mathbf{x}} + (\hat{\mathbf{x}} + i\hat{\mathbf{y}})\alpha]\exp[i(k_o z - \omega_o t)] \tag{7}$$

where α is proportional to the amplitude of the circularly polarized component of the wave defined by

$$\alpha = -\frac{2\omega_{pe}^2\omega_o}{k^2c^2(\omega_o - \Omega_e)} \tag{8}$$

where ω_{pe} and c are the electron plasma frequency and the speed of light in vacuum, respectively, and k is the wave number of the density perturbation defined by (4). Rewriting the scattered field in terms of the ionospheric irregularity scale length, $\lambda = 2\pi/k$, we find

$$\mathbf{E}_s = E_o\exp[ikx](\delta\tilde{n}/N_o)\exp[i(k_o z - \omega_o t)] \times [\underbrace{\hat{\mathbf{x}}}_{LP} + \underbrace{(\hat{\mathbf{x}} + i\hat{\mathbf{y}})}_{CP}\frac{\lambda^2}{\lambda_c^2}] \tag{9}$$

where

$$\lambda_c = \sqrt{2}\pi(c/\omega_{pe})(\Omega_e/\omega_o)^{1/2} \approx 4.4/k_o \tag{10}$$

The scattered field is composed of a linearly polarized (LP) part and a circularly polarized (CP) part as indicated in (9). If the ratio $(\lambda^2/\lambda_c^2) \ll 1$ (i.e., $|\mathbf{k}| \gg |\mathbf{k}_o|$), the scattered wave is dominated by the linearly polarized component which, corresponding to a lower hybrid mode, oscillates in the direction of the irregularity wave vector $\mathbf{k}$; hence, the wave is electrostatic in nature and exhibits a broadened, enlarged wave vector spectrum relative to the incident wave. The

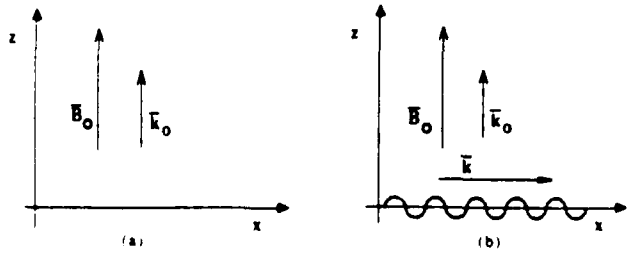

Fig. 1 Geometry of wave propagation for (*a*) uniform ionosphere and (*b*) ionosphere with irregularities.

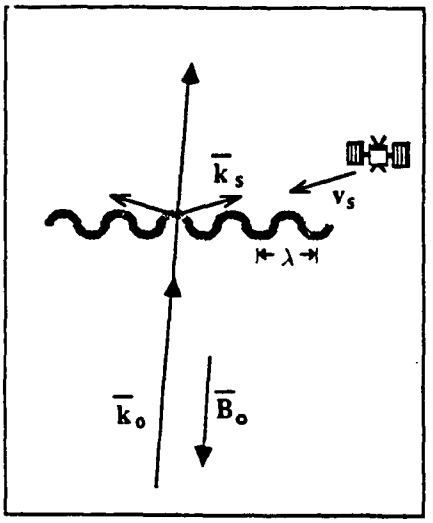

Fig. 2. Schematic of Doppler shift phenomena.

Doppler shift frequency measured by a moving satellite will be enlarged as elaborated in the next section.

Analysis

The condition found above for effective nonlinear scattering into electrostatic modes requires $\lambda \ll \lambda_c$. Typical plasma parameters for the upper ionosphere/lower magnetosphere region of interest are $\omega_{p_e}/2\pi = 0.7$ MHz and $\Omega_e/2\pi = 0.6$ MHz. Assuming an incident frequency of $\omega_o/2\pi = 13.6$ kHz, we calculate $\lambda_c \approx 2$ km. The magnitude of the bandwidth expansion of the scattered VLF wave measured by a moving satellite due to the Doppler shift effect is given by

$$\Delta f = \frac{\mathbf{k}_s \cdot \mathbf{v}_s}{2\pi} \simeq \frac{v_s cos\theta}{\lambda} \approx \frac{v_s}{\lambda} \qquad (11)$$

where $\mathbf{v}_s$ is the velocity of a satellite moving across the Earth's magnetic field as shown in Figure 2, and $\mathbf{k}_s = k\hat{\mathbf{x}} + k_o\hat{\mathbf{z}}$. Given $v_s \simeq 8$ km/s and $\Delta f \simeq 100$ Hz, we find $\lambda \simeq 80$ m $\ll \lambda_c \simeq 2$ km, so the condition for nonlinear scattering is well satisfied. Thus we have found that ionospheric irregularities with scale lengths of several tens of meters can produce Doppler shifts of the observed magnitude. Since $k(\lambda) \gg (\ll) k_o(\lambda_o)$, the simplification made in the formulation of the theory, namely, the assumption that the ducted whistlers propagate exactly along the Earth's magnetic field, is justified. Under this condition, even if the ducted whistlers have nonzero wave normal angles, the formulation of nonlinear scattering mechanism will not be significantly modified.

Ionospheric irregularities can occur naturally. There are many mechanisms that can generate field-aligned iono spheric irregularities [e.g., *Fejer and Kelley*, 1980]. Particle precipitation invoked by *Bell et al.* [1983] can produce irregularities with a broad range of scale lengths in a region near the F layer peak, about 300 km above the Earth's surface. The F region irregularities, as Bell et al. suggested, provide a favorable ionospheric condition for the linear scattering of the VLF waves and the subsequent coupling into quasi-electrostatic whistler wave modes. However, the amplitude of such a quasi-mode wave decreases with distance as it propagates upward to the satellite altitudes of 600–3800 km. This arises from the fact that the electrostatic whistlers are not eigenmodes but quasi-modes of ionospheric plasmas. Therefore, during the ionospheric propagation of quasi-electrostatic whistlers, the ionospheric plasmas do not respond in phase to these quasi-modes. This phase mixing (or phase mismatching) can attenuate the waves significantly during their propagation from the source region to the satellite location.

By contrast, our proposed nonlinear scattering mechanism can produce lower hybrid waves which are eigenmodes of ionospheric plasmas, experiencing less spatial attenuation than the quasi-electrostatic whistler modes during propagation. This mechanism is effective provided that field-aligned ionospheric irregularities exist and that the VLF wave frequency is greater than the local LHR (lower hybrid resonance) frequency. The characteristics of the nonlinear scattering mechanism, then, explain the observed facts that the spectral broadening phenomenon occurs only in the presence of impulsive VLF hiss and/or a LHR noise band with an irregular cutoff frequency, and only for signals whose frequencies exceed the LHR frequency at the satellite location.

3. PARAMETRIC EXCITATION OF LOWER HYBRID WAVES

In this section we discuss the proposed second mechanism responsible for the observed VLF spectral broadening. While the nonlinear scattering mechanism does not work in the absence of ionospheric irregularities, lower hybrid wave modes can be excited parametrically by the VLF waves in the ionosphere. The parametric excitation of lower hybrid waves by the injected VLF waves has been suggested by us [*Lee and Kuo*, 1984] with the following scenario.

Propagating from the neutral atmosphere into the ionosphere, the incident VLF wave can be considered to be a ducted whistler mode with $\mathbf{k}_o = k_o\hat{\mathbf{z}}$ along the geomagnetic field lines, taken to be the z axis of a Cartesian system of coordinates. Assuming the space-time dependence of the perturbations to be $\exp[i(\mathbf{k}\cdot\mathbf{r} - \omega t)]$, the proposed parametric instability can be described by the following wave frequency and wave vector matching relations:

$$\omega_{1+} - \omega_s = \omega_o = \omega_{1-} + \omega_s^* \qquad (12a)$$

$$\mathbf{k}_{1+} - \hat{\mathbf{x}}k_s = \hat{\mathbf{z}}k_o = \mathbf{k}_{1-} + \hat{\mathbf{x}}k_s \qquad (12b)$$

where the subscripts minus/plus and s represent the Stokes/anti-Stokes components of the high-frequency lower hybrid sidebands and the field-aligned zero-frequency mode, respectively. By the definition of (12a), the Stokes and anti-Stokes components refer to the lower hybrid sidebands whose wave frequencies are downshifted and upshifted, respectively, by ω_s with respect to the whistler wave frequency (ω_o). For a purely growing mode (i.e., Re(ω_s)=0), the Stokes and anti-Stokes components of lower hybrid waves are characterized by their wave vectors, shown in (12b), which are the difference and sum of the wave vectors of the whistler and the purely growing mode, respectively. Both the Stokes and the anti-Stokes components of lower hybrid waves have to be considered in this two-dimensional instability process, since $|\mathbf{k}_s| \gg |\mathbf{k}_o|$ and the concomitantly excited low-frequency mode is a purely growing mode. Thus, $|\mathbf{k}_{1+}| \sim |\mathbf{k}_{1-}| \sim |\mathbf{k}_s|$; it is found that the lower hybrid waves have wave vectors large enough to yield the observed spectral broadening due to the Doppler effect.

It should be pointed out that a four-wave rather than a

simpler three-wave interaction process [*Berger and Perkins*, 1976; *Riggin and Kelley*, 1982] is proposed by *Lee and Kuo* [1984]. While the proposed parametric instability has a broad range of VLF (whistler) wave frequency ω_o, the three-wave interaction process [*Berger and Perkins*, 1976] is restricted to a very narrow frequency band, namely, $\omega_{LH} < \omega_o < \sqrt{2}\omega_{LH}$, where ω_{LH} is the lower hybrid resonance frequency. Further, the excited low-frequency mode in the work of *Lee and Kuo* [1984] is a zero-frequency mode. This four-wave interaction mechanism is found to require much lower thresholds than the three-wave interaction mechanism to excite lower hybrid waves in the ionosphere. Based on this proposed four-wave interaction process, we can interpret the observations of the VLF wave-excited lower hybrid waves in the ionosphere indicated in the experiments of the Franco-Soviet ARCAD 3 satellite [*Berthelier et al.*, 1982] and others [e.g., *Chmyrev et al.*, 1976].

At this point, we should comment on the effectiveness of the parametric instability in causing the observed VLF spectral broadening phenomenon. Although the production of lower hybrid waves by the parametric instability does not require the presence of naturally occurring ionospheric irregularities, this mechanism needs a threshold to operate. The thresholds in terms of whistler (VLF) wave electric fields can be calculated from equation (22*b*) of *Lee and Kuo* [1984]:

$$E_m = 0.86(k_s^2 v_{te}^3/\Omega_e)(m/e)|\eta|^{-1/2} \times \left[1 + \left(1 + \frac{4\Omega_e^2\nu_e^2\eta^2}{k_s^4 v_{te}^4}\right)^{1/2}\right]^{1/2} \quad (13)$$

where k, v_{te}, ν_e, and Ω_e are the wave number of field-aligned ionospheric irregularities, the electron thermal velocity, the electron-ion collision frequency, and the electron cyclotron frequency; η is defined by $[1+(M/m)(k_o/k)^2]/[1-(M/m)(k_o/k)^2(\Omega_e/\omega_{pe})^2]$ where M/m, k_o, and ω_{pe} are the ratio of oxygen ion (O^+) mass to electron mass, the wave number of the incident whistler wave, and the electron plasma frequency, respectively. It should be noted that the parametric wave number k is determined by the dispersion relation for the lower hybrid waves, $\omega_o = \omega_{LH}[1+(M/m)(k_o/k_s)^2]^{1/2}$, where ω_{LH} is the lower hybrid resonance frequency defined by $\omega_{LH} = \omega_{pi}/(1+\omega_{pe}^2/\Omega_e^2)^{1/2}$. If we choose the following model parameters: $v_{te} = 1.3 \times 10^6$ (m/s), $\omega_{pe}/2\pi = 0.7$ MHz (i.e., $N_o = 6 \times 10^9$ m^{-3}), $\nu_e = 10$ Hz, $\Omega_e/2\pi = 0.6$ MHz, the threshold field E_m is found to be 18 μV/m. According to *Inan and Bell* [1985], the measured power flux of transmitted VLF signals is 2×10^{-13} W/m^2 at the satellite location; namely, the measured field intensity of whistlers is 12 μV/m, which is of the same order of magnitude as the threshold of the parametric instability. The measured power flux (field intensity) of whistler (VLF) waves in the lower ionosphere is 2×10^{-9} W/m^2 (1.2 mV/m), which is also of the same order of magnitude as the instability thresholds calculated by *Lee and Kuo* [1984]. Therefore, it is possible for the instability to be excited though the VLF transmitters are operated in pulsed mode with a typical duration of seconds.

It is interesting to note that the proposed two source mechanisms are expected to produce broadened VLF spectra with different shapes. The parametric instability will preferentially excite lower hybrid waves with the scale length ($\lambda = 2\pi/k$) of $\sim$ 90 m at the satellite location. This likely generates a two-humped spectrum suppressed at the carrier frequency (f_o) relative to the sidebands peaking at approximately $f_o \pm 100$ Hz, whereas the nonlinear scattering mechanism simply broadens the bandwidth of the injected VLF waves, producing single-peaked spectra. This can be clearly seen from equation (9), showing that the scattered field intensity E_s is the incident field intensity E_o multiplied by the fractional plasma density fluctuation ($\delta n/N_o < 1$). This naturally leads to the broadened VLF spectrum peaking at the carrier frequency. These two types of broadened VLF spectra have indeed been observed. Nevertheless, the single-peaked spectra were much more frequently seen than the double-humped spectra (H. G. James, personal communications, 1988). The characteristics of our proposed two source mechanisms agree well with the observations. Hence, the observations of VLF spectral broadening offer additional evidence supporting the excitation of lower hybrid waves by VLF waves in the ionosphere as suggested by *Lee and Kuo* [1984].

4. SUMMARY AND CONCLUSION

In summary, we have investigated two possible source mechanisms that may be responsible for the observed spectral broadening of injected VLF waves. In the presence of ionospheric irregularities with various scale lengths as short as several tens of meters, the nonlinear scattering of the VLF waves off these density irregularities can produce electrostatic modes with larger wave vectors which give rise to the apparent spectral broadening through the Doppler shift observed by the moving satellites. The amplitude of the electrostatic modes depends linearly on the amplitude of the ionospheric irregularities. The broadening produced through this mechanism is of the same magnitude as the observed values. This mechanism produces single-peaked broadened spectra of VLF waves, which were most frequently observed in the experiments. There are many natural sources that can generate ionospheric irregularities with a broad range of scale lengths, providing favorable ionospheric conditions for the operation of the nonlinear scattering process.

In the absence of ionospheric irregularities, the spectral broadening of the incident wave packet may also stem from the second mechanism, which involves the parametric excitation of lower hybrid waves [*Lee and Kuo*, 1984]. This mechanism requires a threshold that can be exceeded by the employed navigation transmitters. These excited lower hybrid waves have much shorter (larger) wavelengths (wave numbers) than those of the injected VLF waves. The broadening introduced by this mechanism is characterized by the fact that it produces wave frequency spectra that exhibit suppressed field intensity at the carrier frequency and enhanced intensity at a discrete set of frequencies on either side of the carrier frequency. Such spectra are less frequently observed than those produced by the nonlinear scattering mechanism. The lower hybrid waves excited by this mechanism have enlarged wave vectors; the apparent broadening due to the Doppler effect is comparable to that calculated for the first mechanism.

We conclude that the two suggested mechanisms can contribute additively to the observed spectral broadening of injected VLF waves reported by *Bell et al.* [1983] and others. This spectral broadening phenomenon provides additional

evidence to support the mechanism suggested by *Lee and Kuo* [1984] for the excitation of lower hybrid waves by injected VLF (whistler) waves.

Acknowledgments. This work was supported by NASA contract NAG 5-1055, Lincoln Laboratory grant (under the Air Force contract to Lincoln Laboratory F19628-80-C-0002), and the RADC contract through Southeastern Center for Electrical Engineering Education, and the AFOSR grant AFOSR-88-0217 at the Massachusetts Institute of Technology, and by NSF grant ATM-8713217 and AFOSR contract AFOSR 88-0127 at the Polytechnic University. The earlier work by *Lee et al.* [1986] was supported by AFGL contract F19628-83-K-0024. We greatly appreciate the two referees' constructive comments.

The Editor thanks C. L. Siefring and another referee for their assistance in evaluating this paper.

REFERENCES

Bell, T. F., H. G. James, U. S. Inan, and J. P. Katsufrakis, The apparent spectral broadening of VLF transmitter signals during transionospheric propagation, *J. Geophys. Res.*, *88*, 4813, 1983.

Berger, R. L., and F. W. Perkins, On threshold of parametric instabilities near the lower hybrid frequency, *Phys. Fluids*, *19*, 406, 1976.

Berthelier, J. J., et al., Measurements of the VLF electric and magnetic components of waves and dc electric field on board the AUREOL-3 spacecraft: The TBF-ONCH experiment, *Ann. Geophys.*, *38*, 643, 1982.

Chmyrev, V. M., V. K. Roldugin, I. A. Zhulin, M. M. Mogilevskii, V. I. Di, V. K. Koshelevskii, V. A. Bushmarin, and O. M. Raspopov, Artificial injection of very low frequency waves into the ionosphere and the magnetosphere of the Earth, *JETP Lett.*, *29*, 409, 1976.

Fejer, B. G., and M. C. Kelley, Ionospheric irregularities, *Rev. Geophys.*, *18*, 401, 1980.

Gurnett, D. A., and L. A. Frank, VLF hiss and related plasma observations in the polar magnetosphere, *J. Geophys. Res.*, *77*, 172, 1972.

Inan, U. S., and T. F. Bell, Spectral broadening of VLF transmitter signals observed on DE 1: A quasi-electrostatic phenomenon?, *J. Geophys. Res.*, *90*, 1771, 1985.

Laaspere, T., W. C. Johnson, and L. C. Semprebon, Observations of auroral hiss, LHR noise and other phenomena in the frequency range 20 Hz-540 kHz on OGO 6, *J. Geophys. Res.*, *76*, 4477, 1971.

Lee, M. C., and S. P. Kuo, Production of lower hybrid waves and field-aligned density striations by whistlers, *J. Geophys. Res.*, *89*, 10873, 1984.

Lee, M. C., J. F. Kiang, and S. P. Kuo, On the causes of spectral broadening of injected VLF waves (abstract), *EoS Trans. AGU*, *67*, 317, 1986.

McEwen, D. J., and R. E. Barrington, Some characteristics of the lower hybrid resonance noise bands observed by the Alouette I satellite, *Can. J. Phys.*, *45*, 13, 1967.

Riggin, D., and M. C. Kelley, The possible production of lower hybrid parametric instabilities by VLF ground transmitters and by natural emissions, *J. Geophys. Res.*, *87*, 2545, 1982.

K. M. Groves and M. C. Lee, Plasma Fusion Center, NW 16-234, Massachusetts Institute of Technology, Cambridge, MA 02139.

S. P. Kuo, Weber Research Institute, Polytechnic University, Farmingdale, NY 11735.

(Received October 13, 1987;
revised July 19, 1988;
accepted July 27, 1988.)

J. Geomag. Geoelectr., 40, 1141-1145, 1988

Appendix C

Combined Operation of Two Ground Transmitters for Enhanced Ionospheric Heating

M. C. LEE[1], K. M. GROVES[1], C. P. LIAO[1], D. R. RIVAS[1], and S. P. KUO[2]

[1]*Massachusetts Institute of Technology, Cambridge, Massachusetts 02139, U.S.A.*
[2]*Polytechnic University, Farmingdale, New York 11735, U.S.A.*

(Received April 8, 1988; Accepted June 3, 1988)

The combined operation of an HF or MF ground transmitter and a VLF transmitter for enhanced ionospheric heating is discussed. The HF or MF transmitter, operated in a pulsed mode, can preferentially produce short-scale density striations that can render the nonlinear mode conversion of the subsequently launched VLF waves into lower hybrid waves. In addition to the mode conversion process, the VLF waves, if intense enough, can also excite meter-scale density striations and lower hybrid waves via parametric instabilities. Intensified density striations and enhanced airglow are expected, and they can be detected by incoherent backscatter radars and photometers, respectively. The feasibility and planning of the proposed experiments are addressed.

1. Introduction

An experimental scheme is discussed for enhanced ionospheric heating by the combined operation of two powerful ground transmitters. One is an HF or MF heater wave, and the other is a VLF heater wave. The proposed scenario is as follows.

The ionosphere is illuminated by an HF or MF wave first and, then, a VLF wave subsequently (see Fig. 1). It has been known both theoretically and experimentally that short-scale (i.e., less than a few meters) ionospheric irregularities can be excited within seconds by HF heater waves, while it takes tens of seconds or longer for large-scale (say, hundreds of meters and longer) ionospheric irregularities to be generated (see, e.g., GUREVICH, 1978; FEJER, 1979; FREY *et al.*, 1984; COSTER *et al.*, 1985). As shown in Section 2 of this paper, short-scale ionospheric density striations can effectively cause the nonlinear scattering of VLF waves into lower hybrid waves. Hence, we only need to operate the HF or MF heater in pulsed mode to assure the excitation of meter-scale ionospheric irregularities. During the vertical ionospheric heating, the HF heater wave frequencies should be less than the f_0F_2 for overdense heating of the ionospheric F region. When a MF heater is used, the wave frequency is required to match the local electron gyrofrequency in the ionosphere to produce short-scale ionospheric irregularities via electron cyclotron heating (LEE *et al.*, 1986).

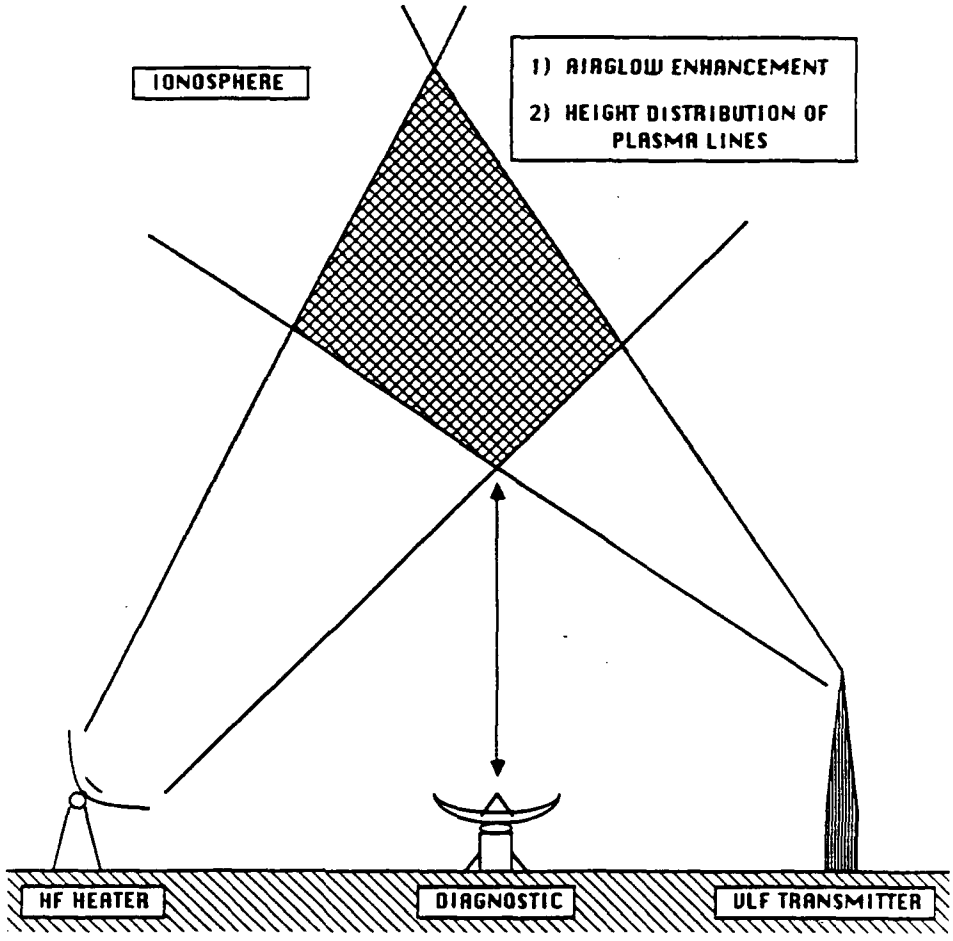

Fig. 1. The proposed experiment for enhanced ionospheric heating: Illumination of the ionosphere by a HF or MF ground transmitter first, and then a VLF ground transmitter subsequently.

In addition to the nonlinear scattering process, the VLF waves, if intense enough, can also excite lower hybrid waves and ionospheric irregularities via parametric instabilities (LEE and KUO, 1984). The suggested diagnoses for the expected ionospheric effects shall be discussed in Section 3. In principal, the two different processes producing the lower hybrid waves can be experimentally distinguished.

2. Heater Wave-Induced Ionospheric Effects

2.1 Mode conversion via nonlinear scattering process

Various plasma instabilities can be excited by HF heater waves during overdense ionospheric heating. In seconds, short-scale ionospheric density striations can be generated concomitantly with Langmuir waves, upper hybrid waves etc. However, it requires tens of seconds for the generation of large-scale ionospheric irregularities by self-focusing instability or thermal filamentation instability. Large-scale irregularities can give rise to phase and amplitude scintillation of beacon satellite signals. These wave interference patterns may not be associated with significant attenuation of the radio signals. By contrast, the short-scale irregularities are able to cause anomalous absorption of the radio signals via the nonlinear scattering process described below that converts electromagnetic wave energy into electrostatic wave energy (eventually, plasma kinetic energy) in the ionosphere.

For simplicity, a ducted whistler (VLF) wave propagating along the $\hat{z}$ direction is assumed, viz.,

$$\boldsymbol{E}_0 = (\hat{x} + i\hat{y})\boldsymbol{E}_0 \exp[i(k_0 z - \omega_0 t)]. \tag{1}$$

Further, short-scale ionospheric irregularities induced by an HF or MF heater wave are represented by

$$\delta n = \delta \hat{n} \exp(iky). \tag{2}$$

Solving the wave equation, we can show that the ionospheric irregularities scatter nonlinearly the circularly polarized (whistler) wave into an elliptically polarized wave. In other words, a linearly polarized component of the scattered wave is introduced by the EM wave-induced field-aligned ionospheric irregularities.

The scattered whistler (VLF) wave field can be expressed as

$$\boldsymbol{E}_s = \{(\hat{x} + i\hat{y})E_{cp} + \hat{y}E_{lp}\} \exp[i(k_0 z - \omega_0 t)], \tag{3}$$

where $E_{cp} = E_0(\delta n / N_0)$ representing the wave field intensity of the circularly polarized component while E_{lp} represents that of the linearly polarized component, N_0 is the unperturbed plasma density. It is found that E_{cp} and E_{lp} are related by

$$E_{cp} = 2\left(\frac{\lambda}{\lambda_0}\right)^2 E_{lp}, \tag{4}$$

where $\lambda = 2\pi / k$ and $\lambda_0 = 2\pi / k_0$ are the scale size of ionospheric irregularities and the wavelength of the whistler wave, respectively. If a VLF wave at the frequency of 10 kHz is injected, and the ionospheric conditions are assumed to be f_c (electron cyclotron frequency)=1.3 MHz and f_p (electron plasma frequency)=6 MHz, the

whistler wavelength in the ionosphere is found to be about 500 meters. According to Eq. (4), E_{lp} dominates over E_{cp} provided that $\lambda \ll \lambda_0$. Hence, meter-scale irregularities produced by HF of MF heater wave can effectively render the nonlinear mode conversion of a VLF (whistler) wave into a lower hybrid wave. The parallel and perpendicular wave vectors of the lower hybrid wave are identical to the wave vector of the ducted whistler wave and that of the field-aligned ionospheric irregularities, respectively.

2.2 VLF wave-excited parametric instabilities

While, in principle, the nonlinear scattering process occurs at any field intensity of the incident VLF wave, parametric instabilities can be triggered by intense enough VLF waves as suggested in LEE and KUO (1984). Short-scale ionospheric irregularities associated with zero-frequency modes can be excited simultaneously with lower hybrid waves by the VLF waves. Therefore, the HF or MF heater wave-induced short-scale ionospheric irregularities can be further strengthened by the VLF heater waves.

3. Diagnoses of Expected Ionospheric Effects

It is generally believed that spread *F* echos in ionograms and scintillation phenomena are caused by large-scale (say, hundreds of meters) ionospheric irregularities. The generation of large-scale ionospheric density irregularities, therefore, can be sensed by ionosondes and scintillation measurements of radio stars or beacon satellite signals. By contrast, the presence of field-aligned short-scale (a few meters and less) irregularities can be detected by backscatter radars.

Backscatter radar measurements can also be made for detecting the excited lower hybrid waves when the radar's beam angle is 90° with respect to the earth's magnetic field. The recorded incoherent backscatter radar spectrum should look like a double-humped ion spectrum peaking at the lower hybrid wave frequency. Since lower hybrid waves can accelerate electrons effectively along the geomagnetic field, airglow enhancement due to the impact excitation of neutrals by energetic electrons can be expected. Measurements of airglow at 6300 Å (red), 5577 Å (green), and even shorter wavelengths may possibly be observed. In addition, the technique described in CARLSON *et al.* (1982) for finding the height distribution of enhanced plasma lines is capable of distinguishing further the electron acceleration by Langmuir waves and/or upper hybrid waves, and lower hybrid waves that are produced, respectively, by HF and VLF heater waves.

There are several ionospheric heating facilities operated at the frequencies of a few MHz in the HF or MF band in the U.S.A., Europe, and the U.S.S.R. VLF transmitters have been used at different locations for the study of wave-particle interactions in the magnetosphere. However, it may not be possible to use the existing HF (or MF) and VLF transmitters for the proposed experiments. Since VLF waves in a narrow frequency band can be generated by lightning storms, the experiments can be carried out with available ionospheric heating facilities during

lightning storms. It is not necessary to have lightning storms occurring nearby. If lightning occurs at the conjugate location in the opposite hemisphere, the lightning-induced VLF waves can propagate in ducted whistler wave modes and bounce back and forth for several cycles before they die out.

This work was supported by NASA contract NAG5-1055, Lincoln Lab grant (under the Air Force Contract to Lincoln Lab # F19628-80-C-0002) and the RADC contract through Southeastern Center for Electrical Engineering Education at the Massachusetts Institute of Technology, and by the NSF grant ATM-8713217 and the AFOSR contract AFOSR 88-0127 at the Polytechnic University. Part of this work was presented in the International Symposium on Modification of the Ionosphere by Powerful Radio Waves, Suzdal Moscow, U.S.S.R., September 9-12, 1986.

REFERENCES

CARLSON, H. C., V. B. VICKWAR, and G. P. MANTAS, Observation of fluxes of suprathermal electron accelerated by HF excited instabilities, *J. Atmos. Terr. Phys.*, **44**, 1089-1100, 1982.

COSTER, A. J., F. T. DJUTH, R. J. JOST, and W. E. GORDON, The temporal evolution of 3-meter striations in the modified ionosphere, *J. Geophys. Res.*, **90**, 2807-2818, 1985.

FEJER, J. A., Ionospheric modification and parametric instabilities, *Rev. Geophys. Space Phys.*, **17**, 135-153, 1979.

FREY, A., P. STUBBE, and H. KOPKA, First experimental evidence of HF produced electron density irregularities in the polar ionosphere; diagnosed by UHF radio star scintillations, *Geophys. Res. Lett.*, **11**, 523-526, 1984.

GUREVICH, A. V., *Nonlinear Phenomena in the Ionosphere* (Physics and Chemistry in Space 10), 370 pp., Springer-Verlag, 1978.

LEE, M. C. and S. P. KUO, Production of lower hybrid waves and field-aligned density striations by whistlers, *J. Geophys. Res.*, **89**, 10873-10880, 1984.

LEE, M. C., J. A. KONG, and S. P. KUO, On the resonant ionospheric heating at the electron gyrofrequency, *Proc. Int. Symp. Modif. Ionos. Powerful Radio Waves*, Suzdal Moscow, U.S.S.R., September 9-12, 1986.

MISSION
of
Rome Air Development Center

RADC plans and executes research, development, test and selected acquisition programs in support of Command, Control, Communications and Intelligence (C^3I) activities. Technical and engineering support within areas of competence is provided to ESD Program Offices (POs) and other ESD elements to perform effective acquisition of C^3I systems. The areas of technical competence include communications, command and control, battle management information processing, surveillance sensors, intelligence data collection and handling, solid state sciences, electromagnetics, and propagation, and electronic reliability/maintainability and compatibility.